

NUMERICAL SIMULATION OF BOILING HEAT TRANSFER

Ying He, Shigeo Maruyama and Masahiro Shoji
Department of Mechanical Engineering, Faculty of Engineering,
The University of Tokyo, Tokyo, Japan

ABSTRACT

It's considered that pool boiling heat transfer is closely related to the intermittent behavior of vapor mass and the consumption of macro-layer on the heated surface. Many experiments have been carried out to support the macro-layer evaporation model, however, little has been done in the numerical simulation of boiling heat transfer. This paper reports a method to simulate heat transfer near the boiling surface by using time dependent dry-patterns of macro-layer. Employing one-dimensional heat conduction model, the processes of heat transfer for nucleate boiling, critical heat flux condition and transition boiling were simulated. In addition, the boiling curve for water and FC-72(C_6F_{14}) were predicted. The predictions agree reasonably well with experimental data. Moreover, the wall temperature fluctuations for different regimes were examined. The change of initial macrolayer thickness with wall superheat was explored. It could be believed that the numerical simulation is useful for understanding the mechanism of boiling heat transfer more clearly.

INTRODUCTION

It's believed that the macro-layer is important to heat transfer in nucleate and transition boiling at high heat flux. There are several modeling efforts which focus on the instabilities in the tiny vapor passages that are postulated to intersperse the liquid-rich macro-layer immediately adjacent to the heater surface.

Historically, macro-layer evaporation model was firstly proposed by Katto & Yokoya(1970). They considered that the evaporation of the macro-layer under the coalesced bubble was the primary mechanism of heat transfer from the surface. In the nucleate boiling regime, the film doesn't dry out. When critical heat flux is reached, the film evaporates away just at the time when the bubble leaves. In the transition-boiling regime, after the film evaporates away, the vapor bubble still hovers, the surface remains dry for a period of time.

Haramura & Katto(1983) and Pan(1989) suggested an alternate CHF theory based on the role of the macro-layer. Their model still retained the basic element of Zuber model that hydrodynamic instabilities dictate the occurrence of

CHF. However, they proposed that the controlling instabilities occurred not at the walls of large vapor columns but rather at the walls of the tiny vapor stems around active nucleate cavities that intersperse the liquid macro-layer on the heater surface itself.

Another representative model was reported by Dhir & Liaw(1989). They deduced an area and time-averaged model from the experimental measurements of void fraction close to the heater surface. They considered that the energy from the wall was conducted into liquid macro/micro layer surrounding the stems and was utilized in evaporation at the stationary liquid-vapor interface. The total length of vapor-liquid interface (periphery of vapor stems) determined the effectiveness of evaporation. The analysis is based on the assumption that all dissipation of liquid occurs on the walls of the vapor stems.

Currently, Shoji & Kuroki (1994) did experimental observations and modeling efforts. They claimed that the formation of the macro-layer for moderately wetting fluids might be a result of the lateral coalescence of bubbles before their escape from the boiling surface. It suggests one way in which active site density might play a role in high heat-flux nucleate boiling and CHF.

Although these models can explain critical heat flux and transition boiling fairly well. They appear to be some discrepancies among them. In order to investigate whether the heat transfer mechanism of nucleate boiling, critical heat flux and transition boiling could be explained by a unified model, Maruyama et al. (1992) presented a model still basing on the theory of evaporation of macrolayer. The model postulated that vapor stems were formed on the active cavity sites in a certain contact angle and the evaporation phenomena also occur at the liquid-vapor interface. The simulated results showed favorable agreements with the spatially averaged and the time averaged model. However, in this model, one of the most important parameters, the macrolayer thickness, was correlated empirically, which affected the prediction of boiling curve greatly.

In this paper, a developed numerical simulation based on the model of Maruyama et al. is presented. In this simulation, we employed the bisection method to obtain the boiling curves without using empirical correlation about macrolayer

thickness. Additionally, we included the analysis of the heater to obtain the temporal variations of wall temperature. Results of this study could be a good supplement to the previous simulation.

METHOD OF NUMERICAL SIMULATION

Fig. 1 shows the schematic of the top and side views of a vapor bubble over a heated surface. In this model, the macrolayer containing vapor stems occupies the region immediately next to the wall. The vapor stems are formed on the active cavity sites. The most important feature of this model is the introduction of a liquid-vapor stem interface evaporation phenomenon, which means that not only does the evaporation occur at the vapor bubble-macrolayer interface but also at the stem interface.

In this study, we assumed that the temperature of heated surface was uniform. From the heater surface heat is conducted into the macrolayer and is utilized in evaporation at the macrolayer-bubble interface. Therefore, the heat balance is written as

$$-\rho_l H_{fg} \frac{d\delta}{dt} = \frac{\lambda \Delta T}{\delta} \quad (1)$$

By the integration of equation (1), the thickness of macrolayer can be given as

$$\delta(t) = \sqrt{\delta_0^2 - 2 \frac{\lambda \Delta T}{\rho_l H_{fg}} t} \quad (2)$$

where λ is heat conductivity of liquid, ρ_l is density of liquid, H_{fg} is latent heat of evaporation, ΔT is wall superheat, and δ_0 is the initial thickness of macrolayer.

The rate of heat transfer from the liquid-vapor stem interface can be written as

$$\begin{aligned} Q &= \int q dA = \int_0^{r_1} q 2\pi r dr \\ &= 2\pi r_0 \lambda \Delta T \frac{1}{\tan \theta} \left[1 + \frac{\delta}{\tan \theta r_0} + \log \left(\frac{\delta}{\delta_m} \right) \right] \end{aligned} \quad (3)$$

where A is the area of the liquid-stem interface. Suppose that heat from the heated surface is conducted into the interface area and is applied in the evaporation at the stem-liquid interface. Meanwhile, The evaporated heat just contributes to the increase of radius of the vapor stem. Therefore, the heat balance can be written as

$$\int q dA = \rho_l H_{fg} A \frac{dr}{dt} \sin \theta \quad (4)$$

where θ is defined as the contact angle according to the

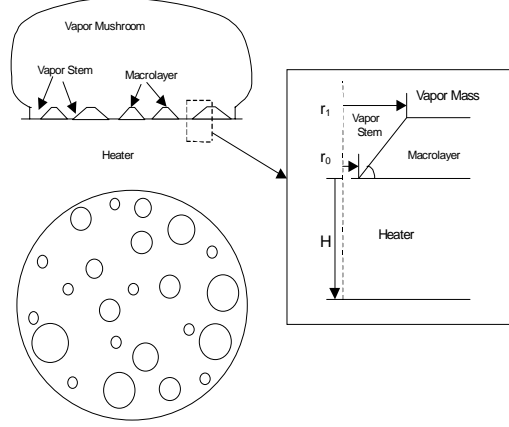


Fig.1. Model of Heat Conduction and Evaporation Near the Liquid-Vapor Interface

model. The growth rate of vapor stems dr_s/dt is then obtained from equation (3) and (4) as

$$\begin{aligned} \frac{dr_s}{dt} &= \frac{1}{\rho_l H_{fg}} \frac{\lambda \Delta T}{\delta} \frac{1}{\tan \theta} \\ &\times \left[\frac{\left(1 + \frac{\delta}{r_0} \tan \theta + \log \left(\frac{\delta}{\delta_m} \right) \right)}{\left(1 + \frac{\delta}{2r_0} \tan \theta \right)} \right] \end{aligned} \quad (5)$$

Because $\frac{\delta}{r_0} \tan \theta \ll 1$, thus equation (5) can be simplified as

$$\frac{dr_s}{dt} = \frac{1}{\rho_l H_{fg}} \frac{\lambda \Delta T}{\delta} \frac{1}{\tan \theta} \left[1 + \log \left(\frac{\delta}{\delta_m} \right) \right] \quad (6)$$

Where δ_m is the thickness corresponding to the maximum evaporated heat for saturated pool boiling of water at atmospheric pressure. The introduction of δ_m is to avoid the infinite heat flux at the liquid-vapor interface. The maximum evaporated heat flux can be obtained by considering the evaporation and condensation of molecules. There exists vapor pressure difference when the surface is at the superheated condition. The mass velocity of evaporated molecules is expressed as

$$\Delta m = \rho_{molec} N v = \rho_v v = \frac{\Delta p}{(2\pi RT)^{1/2}} \quad (7)$$

By Clausius-Clapeyron equation, the relation between pressure difference and superheat can be written as

$$\Delta p / \Delta T = \frac{H_{fg}}{T} \left(\frac{1}{\rho_v} - \frac{1}{\rho_l} \right) \quad (8)$$

The upper limit heat flux thus can be written as

$$q = \Delta m H_{fg} = \frac{\rho_l}{\rho_l - \rho_v} \frac{\rho_v H_{fg}}{T_{sat}} \frac{H_{fg}}{(2\pi RT_{sat})^{1/2}} \Delta T_{sat} \quad (9)$$

For saturated pool boiling of water at atmospheric pressure, the upper limit heat flux can be expressed as

$$q_m = 7.86 \Delta T (MW / m^2) \quad (10)$$

Therefore, δ_m can be expressed from equation (1) as

$$\delta_m = \frac{\lambda \Delta T}{q_m} \quad (11)$$

In order to calculate the instantaneous heat flux q , we introduce a parameter w which is defined as the equivalent thickness. It means the amount of liquid left on the surface. It can be expressed as $w = \delta(1 - \alpha_1)$. Therefore, the instantaneous heat flux can be written as

$$\begin{aligned} q &= \rho_l H_{fg} \left(-\frac{dw}{dt} \right) \\ &= \rho_l H_{fg} (1 - \alpha_1) \left(-\frac{d\delta}{dt} \right) + \rho_l H_{fg} \delta \frac{d\alpha_1}{dt} \\ &= q_{\alpha_1} + q_{\delta} \end{aligned} \quad (12)$$

where q_{α_1} and q_{δ} are heat fluxes related to the decay of macro-layer thickness and the growth of vapor stems. α_1 is the void fraction.

The macrolayer theory considers that the liquid supply occurs periodically and the departure period exactly corresponds to the sustained period of vapor bubble. Using this assumption, we can obtain the averaged heat flux q_{av} at the period. It can be expressed as

$$q_{av} = \frac{1}{\tau} \int_0^{\tau} q dt \quad (13)$$

Because the heat flux is the function of wall superheat, from nucleate boiling to the critical heat flux, for a given heat flux, we can obtain the numerical solution of the corresponding wall superheat by the bisection method. The heat transfer in the transition boiling regime can be explained by the following model

$$q = F q_l + (1 - F) q_v \quad (14)$$

Where F is the fraction of liquid contact, q_b , q_v are the averaged heat flux in nucleate and film boiling regime respectively. According to the above equation, for a given wall superheat, the heat flux can also be obtained by using extrapolated method.

Vapor Stems, Initial Macrolayer and Bubble Departure Period

It's important to determine the values of initial thickness of macro-layer, initial void fraction and bubble departure period before simulating the process of boiling heat transfer near the heated surface. With respect to the initial void fraction, Gaertner (1965) considered that the diameter of the vapor stems had the relationship with the active site population for water as

$$D^2 \frac{N}{A} = \frac{1}{9} \quad (15)$$

where D is the diameter of the vapor stem, N/A is the active site population. Meanwhile, Gaertner & Westwater (1960) concluded the correlation about the active site population as

$$q = 1356 \left(\frac{N}{A} \right)^{0.47} \quad (16)$$

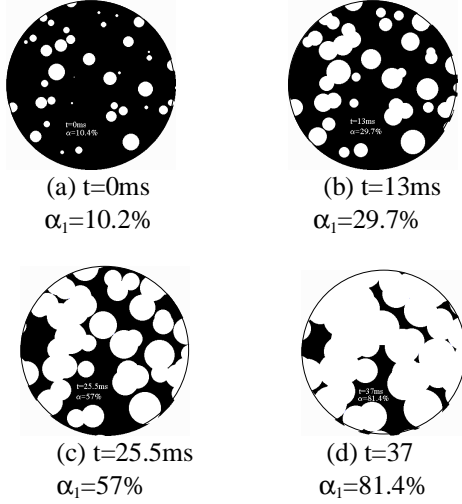
In this simulation, On the basis of the above equations, the active site population was between $8.9 \times 10^5 \sim 1.15 \times 10^6 m^{-2}$.

In general, macrolayer thickness decreases with the increase of heat flux as $\delta \propto q^{-n}$, the n value of available data scatters between 1 and 2. Rajavanshi et al. put forward an equation according to Haramura & Katto's hypothesis, i.e.

$$\delta_0 = 0.0107 \sigma \rho_v \left(1 + \frac{\rho_v}{\rho_l} \right) \left(\frac{\rho_v}{\rho_l} \right)^{0.4} \left(\frac{H_{fg}}{q_{av}} \right)^2 \quad (17)$$

In this simulation, for a given heat flux, the initial macrolayer thickness can be obtained by the above equation. In the transition boiling regime, the extrapolated values of the above equation were employed as the initial macrolayer thickness.

According to Huang's thesis, bubble departure period changes with wall superheat. From the nucleate boiling to critical heat flux, this value almost remains the same. Bubble departure period gradually increases with the decrease of heat flux while entering into the transition boiling region. Regardless of the small increase, we adopted the averaged bubble departure period as 40ms obtained by Katto & Yokoya's equation, i.e.



Figs. 2 Simulated Dry Pattern for CHF

$$\tau = \left(\frac{3}{4\pi} \right)^{\frac{1}{5}} \left[\frac{4(\xi\rho_l + \rho_v)}{g(\rho_l - \rho_v)} \right]^{\frac{3}{5}} v_1^{\frac{1}{5}} \quad (18)$$

Where v_1 is the volumetric growth rate of vapor mass. ξ is the volumetric ratio of the accompanying liquid to the moving bubble.

RESULTS

Fig. 2 is an example of the simulation for saturated pool boiling of water at atmospheric pressure. It shows the growth, coalescence process of vapor stems at CHF condition. The wall superheat is $\Delta T = 30K$. The diameter of the simulated area is set to be 10mm. The contact angle is determined to be 6° . The white parts inside the circle are referred to as vapor stems, and the black parts are referred to as liquid. Fig.2. (a) shows the very beginning state of the simulation with $\alpha_l=10.4\%$. It was formed by producing random number. With the time increases, the macrolayer becomes thinner and the vapor stems become bigger and coalesced. Figs. 2(b)-(d) show the instantaneous near surface pattern within a bubble departure period respectively. It should be noted that at the end of bubble departure period, many isolated liquid areas which were surrounded by vapor stems formed, and the length of periphery of vapor stems seems to be the longest qualitatively.

Fig. 3 showed the simulated boiling curve. The diameter of simulated area was 10mm. As shown, the prediction is reasonable. The simulated critical heat flux is $1.63MW/m^2$ at $\Delta T=30K$. It's in a good agreement with the critical heat flux calculated by the heat balance equation put forward by Katto & Yokoya. The equation is expressed as

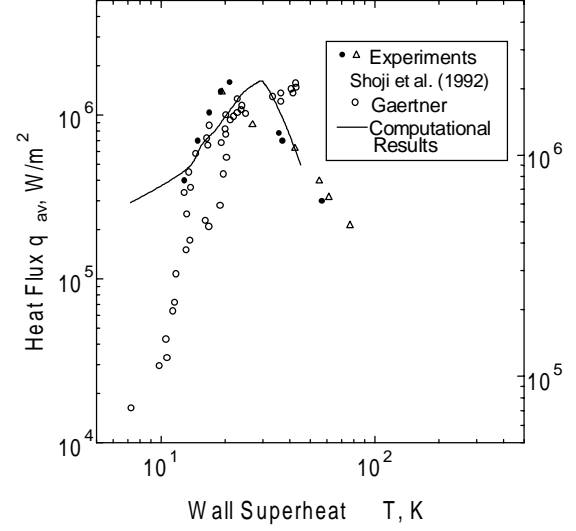


Fig. 3. Simulated Boiling Curve of Water

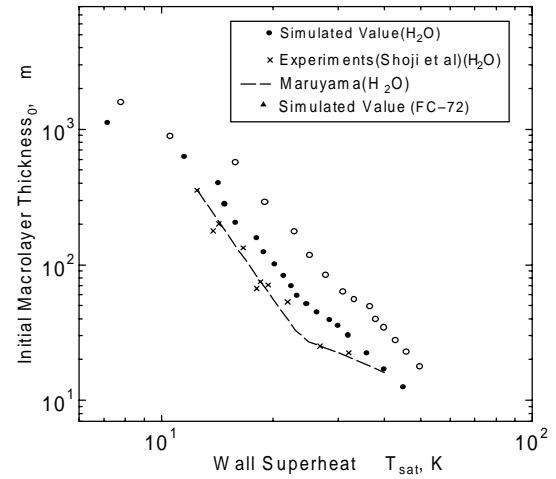


Fig. 4. Simulated Initial Macrolayer Thickness

$$q = \rho_l H_{fg} F \left(1 - \frac{A_v}{A_w} \right) \frac{1}{\tau} \quad (19)$$

Where $F = \delta_0$ for the critical heat flux condition, A_v/A_w is the area fraction of vapor stems.

The relationship between the initial macrolayer thickness and wall superheat is shown in Fig.4. it can be seen that the change of initial macrolayer thickness is closely related to the change of heat flux. Different decreasing rates corresponds to the different boiling regime. Near the critical heat flux condition, the decreasing rate changes considerably, therefore, regime of slugs and columns and transition boiling regime appear.

The boiling curve of FC-72 was also calculated. The fluid was saturated at a temperature of 329K. The bubble departure period τ was calculated by the equation (18).

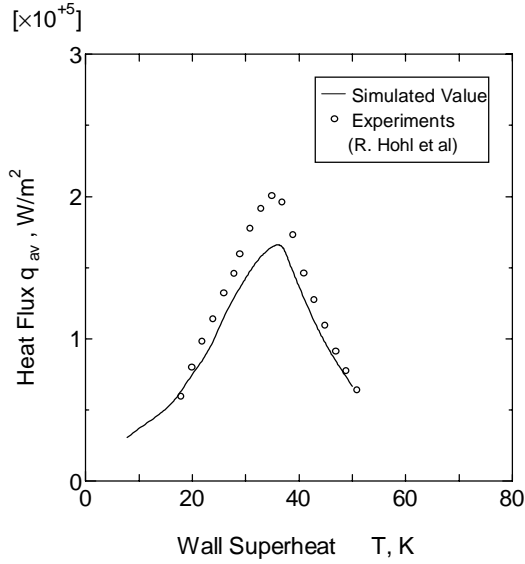


Fig. 5. Simulated Boiling Curve of FC-72

The averaged bubble departure period of FC-72 was then 30ms. The results are plotted in Fig.5. We can see that except the lower critical heat flux, they are almost consistent with the experimental values carried out by Hohl et al. The calculated critical heat flux is $q=1.7 \times 10^5 \text{ W/m}^2$ at $\Delta T=36\text{K}$, whereas the experimental value is $q=2.0 \times 10^5 \text{ W/m}^2$. The lower heat flux than the experimental value may be due to the smaller simulated area of the heater. The experimental heated surface diameter is 34mm.

Temporal Variations in Surface Temperature, Heat Flux and Initial Macrolayer Thickness

The changes of surface temperature are different according to different boiling conditions. The temporal variations in surface temperature were investigated by considered one-dimensional transient heat conduction. As shown in Fig. 1, the heater is copper with 10mm in thickness. The one-dimensional, transient heat conduction in the copper section can be described by the equation

$$\frac{\partial T}{\partial t} = \alpha \frac{\partial^2 T}{\partial x^2} \quad (20)$$

Subjecting to the following initial and boundary conditions

$$t = 0, \quad T_w = T_0 \quad (21)$$

$$x = 0, \quad -\lambda \frac{\partial T}{\partial x} = q_k \quad (22)$$

$$x = H, \quad -\lambda \frac{\partial T}{\partial x} = q_{in} \quad (23)$$

where q_k is the instantaneous heat flux of boiling heat transfer, which can be solved by the built model when

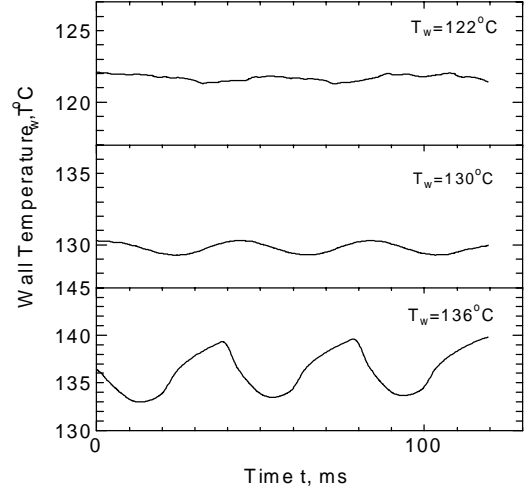


Fig. 6. Temporal Variations in Surface Temperature

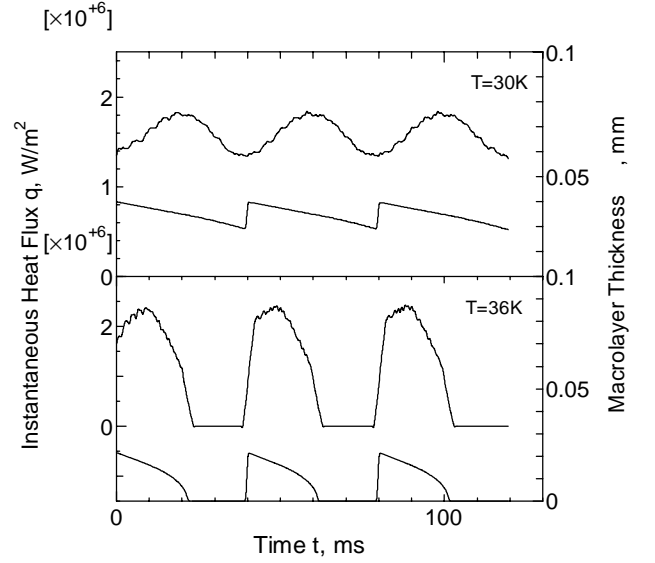


Fig. 7. Temporal Variations of Heat Flux and Macrolayer Thickness

$t \neq 0$. q_{in} is the input heat flux from the bottom of the heater. T_w is the temporal wall temperature and T_0 is the averaged wall temperature corresponding to the input heat flux.

On the other hand, we assumed the macrolayer replenished immediately while the vapor mass departed from the surface despite of the complicity of the transition period. Therefore, used explicit finite difference method, the temporal changes of surface temperature can be obtained. Fig. 6 shows the temporal fluctuations of surface temperature. When the time-averaged temperature is 122K in nucleate boiling regime, the temperature variation is very small, because the surface may be always covered by very thick macrolayer. When reaching to the critical heat flux condition, the change becomes slightly larger, whereas in

the transition boiling regime, the temperature fluctuation become so big that the range reaches several Kelvin. This may be due to that the macrolayer in this regime is considerably thin, the heat fluxes related to the decay of macrolayer thickness and the growth of vapor stems are very big within a short period, thence the surface remains dry for a time before the vapor mass departs. This is in a good agreement with Huang's measurements.

The periodic fluctuations of instantaneous heat flux and initial macrolayer thickness are plotted in Fig.7. The top of the figure shows the change pattern at CHF condition. We can see that the heat flux increases with time, in the middle of the cycle, it reaches the peak value, then deceases gradually until the vapor bubble departs. The macrolayer is considerable thin, at the end of bubble departure period, there's still left over a little amount of liquid. This means that the vapor mass departs before the macrolayer dries out. This shows no difference with the measurements of Kirby & Westwater. The lower part of the figure shows the pattern in the transition boiling regime. The instantaneous heat flux changes violently rather than remains constant before the surface becomes dry.

SUMMARY AND CONCLUSIONS

1. In this study, we developed a method of numerical simulation of boiling heat transfer according to Maruyama's model, which is also based on the theory of macrolayer evaporation. By used heat flux controlled method, the near-surface pattern, which is the growth, coalescence process of vapor stems for nucleate and transition boiling, were simulated. In addition, the boiling curves of water and FC-72 were obtained. Both of them show good results.

2. Considering one-dimensional transient heat conduction, we calculated the surface temperature. Because the characters of macrolayer are varied in different boiling regimes, the corresponded temporal variations in surface temperature changes greatly. Besides this, the temporal variations of heat flux and macrolayer thickness were obtained.

3. In this simulation, the averaged heat fluxes in transition boiling regime were obtained through using the extrapolated values of achieved nucleate boiling curve. Although the method is reasonable and the values are roughly consistent with the available data, more effective method should be investigated in detail.

4. In this model, we assumed that the surface temperatures were uniform spatially. It has been known that spatial variations in surface temperature may not be overlooked. We can also combine the transient heat conduction and boiling heat transfer to calculate the spatial variations, although it may become complicated.

5. The contact angle was set at 6° in this study. It seems a little small, on the other hand, it implies that the microlayer evaporation may also play a role besides the evaporation of

macrolayer from the nucleate boiling to transition boiling.

NOMENCLATURE

q	gravitational acceleration, m/s^2
H_{fg}	Latent heat of vaporization, J/kg
q	instantaneous heat flux, W/m^2
q_{av}	time averaged heat flux, W/m^2
Q	heat transfer rate, W
r_s	radius of a vapor stem, m
r	radial coordinate from the center of a vapor stem, m
α	void fraction
δ	macrolayer thickness, m
δ_0	initial thickness of macrolayer, m
q_m	Gambill-Lienhard upper limit heat flux, W/m^2
δ_m	macrolayer thickness corresponded to q_m , m
α	thermal diffusivity, m^2/s
σ	surface tension, N/m
τ	bubble departure period, s
λ	thermal conductivity, W/mK
θ	contact angle
ρ_{molec}	mass of a molecule
ρ_l	density of liquid, kg/m^3
ρ_v	density of vapor, kg/m^3
t	time, s
T_w	surface temperature, $^\circ C$
N	number of molecules per volume
R	ideal gas constant, J/kgK
v	mean velocity of molecules, m/s

REFERENCES

- Dhir, V. K., and Liaw, P., 1989, "Framwork for Unified Model for Nucleate and Transition Pool Boiling," *Trans. ASME, J. Heat Transfer*, Vol. 111, No.3, pp.739-746.
- Gaetner, R. F., and Westwater, J. W., 1960, "Population of Active Sites in Nucleate Boiling Heat Transfer," *Chem. Eng. Prog. Symp.*, Ser. 56.
- Gaertner, R. F., 1965, "Photographic Study of Nucleate Pool Boiling on a Horizontal Surface," *ASME, J. Heat Transfer*, Vol. 87, pp.17-29.
- Haramura, Y., and Katto, Y., 1983, "A New Hydrodynamic Model of Critical hat Flux, Applicable Widely to Both Pool and Forced Convection Boiling on Submerged Bodies in Saturated Liquids," *Int. J. Heat Mass Transfer*, Vol. 26. No. 2, pp. 389-399.
- Hohl, R., Auracher, H., and Blum, J., 1997, "Identification of Liquid-Vapor Fluctuations Between Nucleate and Film Boiling in Natural Convection," *Convective Flow and Pool Boiling Conference*, Section II: Pool Boiling, Kloster Irsee.
- Huang, Z. L., 1993, "A Study of Steady Transition Boiling of Water," *Ph. D thesis, Faculty of Engineering, The University of Tokyo*.
- Katto, Y., Yokoya, S., and Yasunaka, M., 1970,

“Mechanism of Boiling Crisis and Transition Boiling in Pool Boiling,” *Proc. 4th Int. Heat Transfer Conf.*, Paris, vol.5, pp. B3.2.

Katto, Y., and Yokoya, S., 1975, “Behavior of A Vapor Mass in Saturated Nucleate and Transition pool Boiling,” *Trans. JSME*, Vol. 41, pp.294-305.

Kirby, D. B., and Westwater, J. W., 1965, “Bubble and Vapor Behavior on a heated Horizontal Plate During Pool Boiling Near Burnout,” *Chem. Eng. Prog. Symp.*, Ser.61.

Kutateladze, S. S., 1948, “on the Transition of Film Boiling under Natural Convection,” *Kotloturbostroenie*.

Maruyama, S., Shoji, M., and Shimizu, S., 1992, “A Numerical Simulation of Transition Boiling Heat Transfer,” *Proceedings of the 2nd JSME-KSME Thermal Eng. Conf.*

Pan, C., Hwang, J. Y., and Lin, T. L., 1989, “The Mechanism of Heat transfer in Transition Boiling,” *Int. J. Heat Mass Transfer*, Vol.32, pp.1337-1349.

Pasamehmetaglu, K. O., Chappidi, P. R., Unal C., and Nelson, R. A., 1993, “Saturated Pool Nucleate Boiling Mechanism at High Heat Fluxes,” *Int. J. Heat Mass Transfer*, Vol. 36, No. 15, pp.3859-3868.

Rajvanshi, A. K., Saini, J.S., and Prakash, R., 1992, “Investigation of Macrolayer Thickness in Nucleate Pool Boiling at High Heat Flux,” *Int. J. Heat Mass Transfer*, Vol.35, No. 2, pp. 343-350.

Sadasivan, P., Unal, C., and Nelson, R. A., 1995, “Perspective: Issues in CHF Modeling – The Need for New Experiments,” *Trans. ASME, J. Heat Transfer*, Vol. 117, pp.558-567.

Shoji, M., 1992, “Study of Steady Transition Boiling of Water: Experimental Verification of Macrolayer Evaporation Model,” *Pro. Eng. Found. Conf. Pool External Flow Boiling*, Publ. by ASME, pp.237-242.

Shoji, M., and Kuroki, H., 1994, “Model of Macrolayer Formation in Pool Boiling,” *Pro. 10th Int. Heat Transfer Conf.*, pp. 147-152.

Shoji, M., 1990, “saturated Pool Boiling and Heat Transfer in High Heat Flux regime,” *Pro. 2nd Typical Workshop, JSHT*, pp.66-70.